Brazilian Journal
of Chemical
Engineering

ISSN 0104-6632
Printed in Brazil
www.abeq.org.br/bjche

Vol. 36, No. 01, pp. 201 - 208, January - March, 2019
dx.doi.org/10.1590/0104-6632.20190361s20170498

A FAIR COMPARISON BETWEEN BISMUTH CATALYSTS FOR APPLICATION IN PHOTODEGRADATION UNDER VISIBLE AND SOLAR LIGHT

Camila S. Ribeiro[1*], Milena D. Brandestini[1],
Celso C. Moro[2] and Marla A. Lansarin[1]

[1] Universidade Federal do Rio Grande do Sul, Departamento de Engenharia Química, Porto Alegre, RS, Brasil.
E-mail: camilasr@enq.ufrgs.br, ORCID: 0000-0001-9535-5434; ORCID: 0000-0001-6835-3134
[2] Universidade Federal do Rio Grande do Sul, Instituto de Química, Porto Alegre, RS, Brasil.

(Submitted: September 27, 2017 ; Revised: April 3, 2018 ; Accepted: April 9, 2018)

Abstract - Three different bismuth catalysts (Bi_2WO_6, BiOI and $BiVO_4$) were synthesized using solvo- and hydrothermal methods. Different reaction times, calcination and the addition of poly (vinyl pyrrolidone) during synthesis were tested to investigate the effect of these variables on the catalysts' morphology and photocatalytic activity. The photocatalytic activity was evaluated using the degradation of rhodamine B dye under both visible light and natural solar radiation. The Bi_2WO_6 samples presented good crystallinity and morphological similarities, despite having undergone different treatments. The BiOI and Bi_2WO_6 catalysts presented a spherical shape, and no morphological difference was observed as a result of the addition of PVP. The $BiVO_4$ sample presented a parallelepiped shape. BiOI containing PVP and ethylene glycol was the catalyst that presented the highest activity, while $BiVO_4$ presented the lowest. In experiments using scavengers, photogenerated holes demonstrated a key role in dye degradation.
Keywords: Semiconductors; Bismuth; Photocatalysis; Visible light; Solar light.

INTRODUCTION

Heterogeneous photocatalysis, an Advanced Oxidation Process (AOP) considered to be a sustainable and low operating cost technology, is a suitable wastewater treatment process for effluents containing refractory organic compounds. However, until now, the most common catalysts used in this process are mainly active under UV light, which makes up only about 4% of the sunlight spectrum (Sivakumar et al., 2014; Issarapanacheewin et al., 2016; Meng and Zhang, 2016). Therefore, in order to maximize the effect of solar radiation, it is necessary to develop catalysts that are active under visible light irradiation.

In this context, the use of bismuth-based catalysts has attracted great attention because the hybridization of O - 2p and Bi - 6s levels generates semiconductors with smaller band-gap and a more disperse valence band (VB). This largely disperse VB favors the mobility of the photo holes and is useful for oxidation reactions (Kudo and Hijii, 1999). Furthermore, bismuth is considered to be a non-toxic and low-cost material (Bonné et al., 2017; Kim et al., 2017).

Among various types of bismuth-based catalysts, three stand out: (*i*) bismuth oxyhalides, BiOX (X = Cl, Br, I), ternary compounds that present a tetragonal crystal structure, characterized by Bi_2O_2 slabs interleaved by double slabs of halogen atoms (Qin et al., 2013; Mera et al., 2016; Natarajan et al., 2016);

* Corresponding author: Camila S. Ribeiro - E-mail: camilasr@enq.ufrgs.br

(ii) Bi_2WO_6 (bismuth tungstate), an Aurivillius oxide that has a layered structure with a perovskite-like slab of WO_6 (Ge and Liu, 2014; Liu, Y. et al., 2015; Huang et al., 2016; Kaur and Kansal, 2016); and (*iii*) $BiVO_4$ (bismuth vanadate) in its monoclinic scheelite crystalline form (Dong et al., 2014; Lu et al., 2015; Zhao et al., 2016; Guang et al., 2017).

The photocatalytic activity of these catalysts has been widely studied and improved through various methods. Among them are hydro/solvothermal (Hu et al., 2014; Lin et al., 2014; Wu, D. et al., 2016), sol-gel (Wu et al., 2010; Zhang et al., 2010a; Zhang et al., 2010b), ultrasound (Zhou et al., 2006; Zhou et al., 2007; Dong et al., 2014) and coprecipitation (Alfaro and Martínez-De La Cruz, 2010; Ravidhas et al., 2015). The hydro/solvothermal method is the most widely used, primarily due to its low cost, simplicity, low temperatures and short reaction time. Furthermore, factors that affect the catalyst's activity such as morphology, crystal structure and band gap can easily be controlled by this method.

Although there are several published studies, to the best of our knowledge a fair comparison of photocatalytic activity between different types of bismuth catalysts under the same experimental conditions has not yet been done.

Therefore, in this work, hydro/solvothermal methods were used in the synthesis of three different bismuth catalysts: Bi_2WO_6, BiOI and $BiVO_4$. The relation between the synthesis conditions and the photocatalytic activity of the material obtained was investigated using rhodamine B (RhB) dye. The evaluated variables were: synthesis time, calcining and the addition of polyvinylpyrrolidone (PVP) to Bi_2WO_6 and BiOI.

EXPERIMENTAL

All chemicals were of analytical grade and used as received. The following reagents were used: $Bi(NO_3)_3.5H_2O$ (Sigma-Aldrich), $Na_2WO_4.2H_2O$ (Sigma-Aldrich), ethylene glycol (Fluka), HNO_3 (Synth), KI (Química Moderna), $NaVO_3$ (Fluka), EDTA (Merck), TiO_2 (P25 Evonik), ethanol (Dinâmica), isopropanol (Neon) and RhB (Próton Química). All solutions were prepared with deionized water.

Synthesis of Bi_2WO_6

The typical synthesis was based on the work of Zhang et al. (2007a), in which 0.98 g of $Bi(NO_3)_3.5H_2O$ was dissolved in 30 mL of 0.4 M nitric acid solution. The mixture was then stirred for several minutes at 40 °C. A white precipitate was formed when 20 mL of a 0.05 M Na_2WO_4 (with or without 0.15 g PVP K30) solution was added dropwise into the mixture. After being stirred for 24 hours, the suspension was added to a 70 mL Teflon –lined autoclave and maintained at 160 °C for 8, 16, 24 and 48 hours. The resulting powders were collected, washed with deionized water and dried in an oven at 80 °C. Calcination, when performed, occurred at 500 °C for 2 hours. Calcined samples, containing PVP, were submitted to 16 h in the autoclave.

Synthesis of BiOI

In the synthesis of the BiOI samples, based on Hu et al. (2014), 0.004 mol of $Bi(NO_3)_3.5H_2O$ was poured into 40 mL of ethylene glycol (EG). Next, another 40 mL of the corresponding solvent solution, containing 0.004 mol KI (solution A), was added. The mixture was further stirred for 30 minutes, placed in a 70 mL Teflon –lined autoclave and kept at 160 °C for 16 hours. In the synthesis with PVP, 0.15 g PVP K30 was added to solution A. The synthesized precipitates were washed with ethanol, ethanol/water and water (separately and in this order) and dried in an oven at 60 °C for 12 hours.

Synthesis of $BiVO_4$

The $BiVO_4$ samples were synthesized according to Ma et al. (2015). Solution A contained 6.0 mmol of $Bi(NO_3)_3.5H_2O$ dissolved in 20 mL of 4 M HNO_3. Solution B consisted of 6.0 mmol of $NaVO_3$ and 3.0 mmol of EDTA dissolved in 20 mL of 4 M NaOH. Both were stirred until total dissolution was achieved. Then, solution B was added dropwise into solution A and the pH was adjusted to 7, using a NaOH solution. After further stirring for 30 minutes, the mixture was transferred into a 70 mL Teflon –lined autoclave and maintained at 160 °C for 4 hours. The sample was washed in the same way as the BiOI samples and dried in an oven at 100 °C for 3 hours.

Characterization

The catalysts were characterized by scanning electron microscopy (SEM, JEOL JSM 6060), operating at 10 kV. The X-ray diffraction data were detected via a D500 Siemens diffractometer, using CuKα (λ = 0,154056 nm) radiation. The operating conditions were controlled at 40 kV and 1.75 mA. The UV–vis diffuse reflectance spectra of the samples were recorded with an UV–vis spectrophotometer (Cary 5000 Scan Spectrophotometers, Varian). Nitrogen adsorption–desorption measurements were conducted at 77 K on a Tristar II Krypton 3020 Micrometrics®. The surface area and the volume were calculated based on Brunauer–Emmett–Teller (BET) and BJH (Barret, Joyner and Halenda) analyses.

Photocatalytic experiments

The photocatalytic activity of the bismuth catalysts was evaluated by studying the degradation

of rhodamine B dye (RhB) in an aqueous solution (Figure 1), under 600 W m^{-2} visible light irradiation, using a LED lamp (Stellatech 13 W) as a light source or under natural solar light (Porto Alegre, Brazil, 30° 01' S and 51° 13' W). In each experiment, 50 mg of photocatalyst were added to a 50 mL RhB solution (25 or 50 mg L^{-1}). The experiments were divided into two steps: 1 hour in the dark (30 min in ultrasound and 30 min in magnetic stirring) to ensure the adsorption/desorption equilibrium and 90 minutes of reaction. At given time intervals, 1 mL suspensions were sampled and centrifuged to remove the photocatalyst powders. The RhB concentration was analyzed through a UV–vis spectrophotometer (λ_{max} = 553 nm). In order to determine the role that the •OH radical and the h^+ hole play in the reactions, isopropanol and EDTA were used as scavengers. All experiments were carried out in duplicate or triplicate, when necessary, and average values used as results.

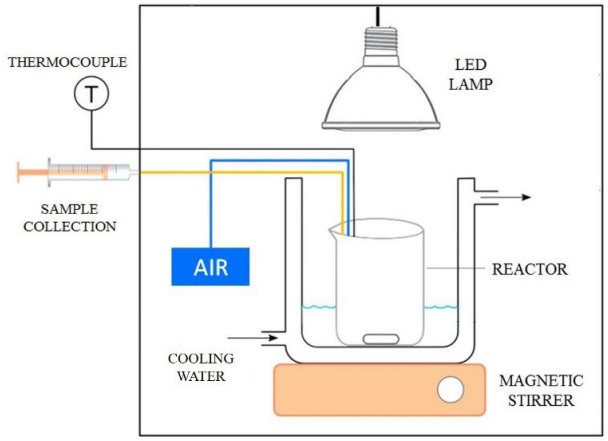

Figure 1. Schematic representation of reactor used in the degradation tests.

RESULTS AND DISCUSSION

Catalysts Characterizations

Morphology and crystalline phase

The SEM images for the Bi_2WO_6 catalysts, Figure 2(a-e), show that all samples have a uniform spherical shape with an approximate average diameter between 6 and 8 μm. Different treatments had little change on the samples' morphology and on the average size of the formed spheres. This fact reveals that there is not necessarily a direct relation between synthesis time and an increase in the microsphere organization, leading to flower-like structures, as reported in the literature (Yu et al., 2005; Zhang et al., 2007; Zhang. et al., 2013). Furthermore, adding PVP did not cause any significant alteration in the samples' morphology (Figure 1f).

The images of the BiOI samples (Figure 2g-h), in turn, showed that microspheres with an approximate average diameter between 2 and 4 μm are obtained in

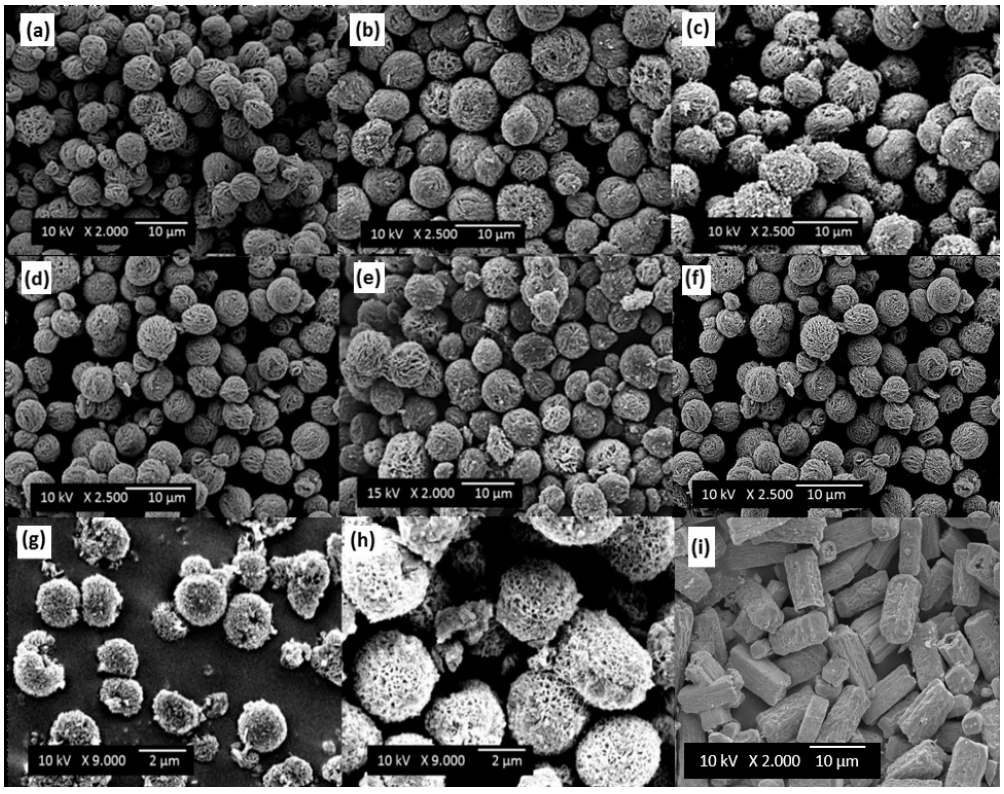

Figure 2. SEM images of bismuth samples: (a) Bi_2WO_6 - 8h, (b) Bi_2WO_6 – 16h, (c) Bi_2WO_6 – 24h, (d) Bi_2WO_6 – 48h, (e) Bi_2WO_6 – 16h - calcined at 500 °C for 2 hours, (f) Bi_2WO_6 - 16h – PVP, (g) BiOI – EG, (h) BiOI – EG – PVP and (i) $BiVO_4$.

the presence of EG as a solvent. The addition of PVP to the BiOI samples - similarly to what occurred with the Bi_2WO_6 samples - produced no significant effect on the size and morphology of the microspheres.

In the case of the $BiVO_4$, the sample showed a three-dimensional structure similar to a parallelepiped (Figure 2i). These parallelepipeds had a roughened surface and an average length between 10 and 12 μm and a width of 5 μm, approximately.

The catalysts' phase and composition were determined by X-Ray diffraction, which demonstrated that all samples presented good crystallinity (Figure 3). Furthermore, it was observed that the main diffraction peaks of the Bi_2WO_6 – 16h (Figure 3a) and BiOI – EG (Figure 3b) samples were associated with the orthorhombic (JCPDS card No. 39-0256) (Lin et al., 2014) and tetragonal phase (JCPDS No. 70-2062) (Xia et al., 2011), respectively. The $BiVO_4$ sample (Figure 3c), however, indicated the presence of peaks characterized by two crystalline phases: monoclinic and tetragonal (JCPDS No. 70-0688 and No. 70-013, respectively) (Zhang et al., 2006; Zhu et al., 2012).

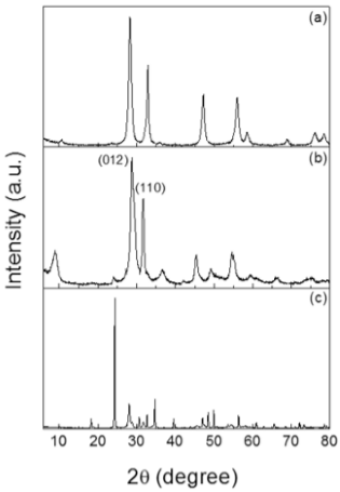

Figure 3. XRD patterns of (a) Bi_2WO_6 -16h, (b) BiOI – EG and (c) $BiVO_4$.

Table 1 provides the specific area, volume, average pore diameter and band gap energy values for the catalysts synthesized in this work. With regards to the Bi_2WO_6 samples, significant area and volume differences were noticed only when the catalyst was subjected to calcination. Furthermore, the PVP addition increased the sample specific surface area by approximately 40%.

BiOI revealed a mesoporous concentration between 2 and 12 nm for the BiOI-EG-PVP sample and a wider distribution, between 5 and 30 nm, for the BiOI – EG. The smaller size of the pores contributed to a larger area for the BiOI-EG-PVP.

Overall, it was observed that the samples with spherical shapes (Bi_2WO_6 and BiOI) had larger surface areas than the parallelepiped shape. For photocatalysis, the catalyst surface area plays an important role, since, in most cases, the larger the illuminated area, the greater the observed number of active sites and degradation.

The optical properties of the samples are shown in Figure 4 and the calculated results are presented

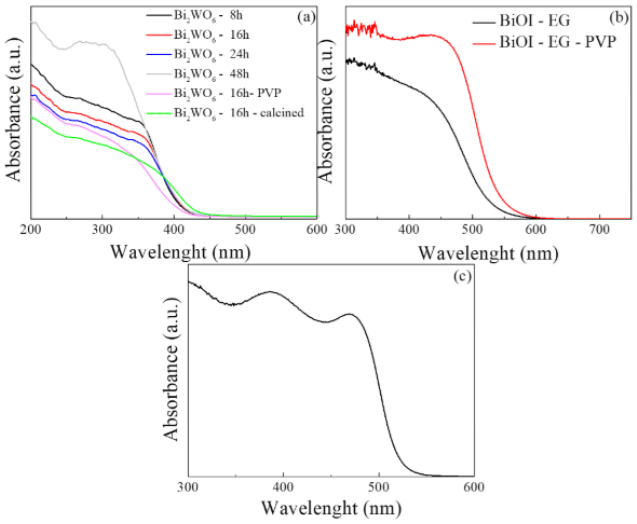

Figure 4. UV–vis diffuse reflection spectra of different catalysts and samples: (a) Bi_2WO_6, (b) BiOI and (c) $BiVO_4$.

Table 1. Surface area, volume, medium diameter, band gap, dark adsorption values and the apparent first-order rate constants (k_{ap}) of different bismuth samples.

Sample	Surface Area ($m^2\ g^{-1}$)	Volume ($cm^3\ g^{-1}$)	Diameter (nm)	Band Gap (eV)	Adsorption (%)	RhB degradation after 90 min (%)	k_{ap} (min^{-1})	R^2
A - Bi_2WO_6 – 8 h	17.7	0.04	6.6	2.90	18.7	46 ± 2	0.0066	0.996
B - Bi_2WO_6 – 16 h	17.8	0.04	6.4	2.96	24.3	63 ± 2	0.0107	0.992
C - Bi_2WO_6 – 24 h	15.6	0.04	6.8	2.94	20.7	55 ± 3	0.0090	0.995
D - Bi_2WO_6 – 48 h	15.2	0.05	9.9	3.05	19.5	51 ± 2	0.0081	0.997
E - Bi_2WO_6 – 16 h – PVP	25.5	0.09	13.2	2.98	23.3	65 ± 2	0.0110	0.997
F - Bi_2WO_6 – calcined (500 °C)	2.2	0.01	19.6	2.84	7.0	12 ± 1	0.0012	0.918
G - BiOI–EG	33.9	0.14	12.8	2.32	74.3	70 ± 1	0.0130	0.998
H – BiOI –EG–PVP	47.5	0.12	7.3	2.27	84.0	85 ± 1	0.0207	0.999
I – $BiVO_4$	9.2	0.03	10.7	2.36	2.5	13 ± 1	0.0013	0.914

in Table 1. It was observed that all samples can be activated by visible light ($\lambda \geq 400$ nm).

Photocatalytic performance

(a) LED lamp

The degradation kinetics of rhodamine B were investigated using the synthesized catalysts, and the experimental results set to a first order kinetics. The degradation after 90 minutes and the (apparent kinetic constant - min^{-1}) values calculated are shown in Table 1.

Preliminary tests showed that direct dye photolysis (degradation only caused by radiation) is about 18%. When comparing the Bi_2WO_6 - 8 and 16 hour samples, it was observed that increasing the sample's time in the autoclave leads to an increase in dye degradation from 46% to 63%. Autoclave times greater than 16 hours resulted in reduced rhB degradation, but still higher than the 8 hour sample. The difference in activity, however, cannot yet be explained and further analyses are necessary in order to clarify these results. For example, in the work of Zhang. et al. (2013), after a photoluminescence analysis, the authors noticed that catalysts synthesized at different times presented distinct lifetimes of photogenerated electron–hole pairs, which explained the different photocatalytic performance.

When adding PVP to the synthesis of Bi_2WO_6, it is noted that the surfactant does not influence rhB degradation. This finding contradicts reports in the literature in which the PVP addition promoted the formation of more organized structures with greater number of active sites and, thus, with more activity (Li et al., 2007; Wu. et al., 2007; Dai et al., 2010). Still, it is clear that calcination affects the catalyst performance by greatly reducing the specific area.

For the BiOI catalysts, no significant morphological change was noted. However, the presence of PVP clearly increases the BiOI photocatalytic activity. The reason, as seen, is because the presence of surfactant increases the surface area, thus increasing the amount of active sites available for the reaction.

The $BiVO_4$ catalyst showed inferior photocatalytic performance when compared to photolysis alone. Therefore, the presence of the catalyst actually has a negative influence on the dye degradation. This result can be attributed to the lower surface area of this catalyst and the presence of the tetragonal crystalline phase. It has been demonstrated that only the monoclinic phase has good photocatalytic activity (Yang et al., 2009).

In general, there is a linear correlation between the illuminated area and the photocatalytic activity, as can be seen in Figure 5a. The figure compares the results of this study with literature data, confirming the importance of obtaining catalysts with larger areas. However, when comparing the band gap values and the total reduction achieved, no correlation was observed (Figure 5b). So, smaller band gap energy does not necessarily imply greater photocatalytic activity. Of course, the band gap determines the wavelength that will activate the catalyst, but once activated, other characteristics will determine the catalyst efficiency in the degradation of certain chemical species.

During the experiments, it was observed that the higher the rhodamine B adsorption on the surface, the greater the activity (Table 1). Those results suggest that the photogenerated holes have a key role in the degradation process. In order to verify this hypothesis, experiments were performed in the presence of isopropanol (IP) (Gamage Mcevoy et al., 2014) and EDTA (Huo et al., 2012), which act as •OH (hydroxyl radical) and h^+ (hole) scavengers, respectively. The concentrations of IP and EDTA in the reaction system were 0.01 M. For the purposes of these tests, the samples with better photocatalytic activity in earlier experiments were chosen. The results are presented in Figure 6. The presence of IP did not result in effective inhibition of the degradation of rhodamine B, showing that the hydroxyl radical does not play an important role in dye degradation. On the other hand, the addition of EDTA clearly hampered the catalyst performance by suppressing the holes, indicating that h^+ plays a key role in the rhodamine B degradation mechanism.

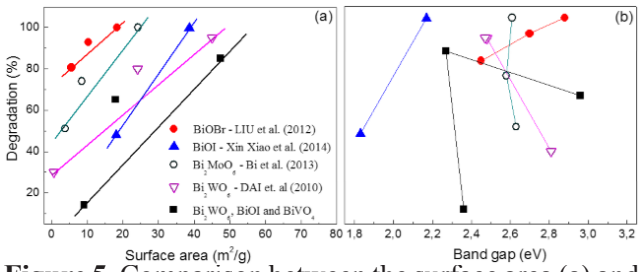

Figure 5. Comparison between the surface area (a) and band gap (b) and photodegradation for several bismuth catalysts (Dai et al., 2010; Liu, Z. et al., 2012; Bi et al., 2013; Xiao et al., 2014) and this work.

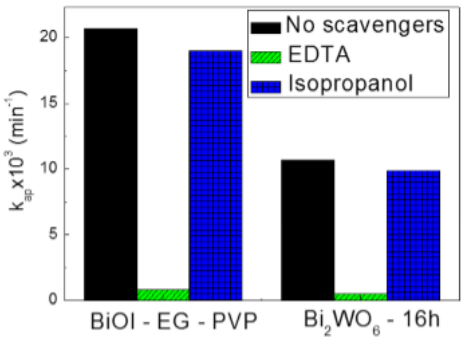

Figure 6. Reaction rate constants for photocatalytic degradation of rhB on BiOI-EG-PVP and Bi_2WO_6 - 16h with and without scavengers.

Table 2. Apparent first-order rate constants (k_{ap}) of different samples under visible and natural solar light.

Sample	Led lamp		Solar light			
	k_{ap} (min^{-1})	R^2	k_{ap} (min^{-1})	R^2	Average UV Radiation ($mW\ cm^{-2}$)	Average visible radiation ($W\ m^{-2}$)
Bi_2WO_6 – 16h	0.0107	0.992	0.0396	0.966	1.36	1085
BiOI - 16h – PVP	0.0207	0.999	0.0308	0.999	1.15	890

(b) Natural solar light

In order to measure the behavior of the synthesized catalysts in the presence of solar radiation, experiments were carried out using the samples that obtained the best results with a LED lamp (Table 2). However, as the experiments were performed on different days, natural interferences did not provide the same irradiation conditions for all the tests. Therefore, a comparison of the different catalysts was not possible. Comparing light sources, however, shows that both catalysts were more efficient in the presence of solar radiation, reaching 94% and 98% rhodamine B degradation for BiOI and Bi_2WO_6, respectively. This result is attributed to the higher radiation incidence on the catalysts, since the sun irradiates in a more energetic range than the LED lamp.

In addition, as can also be observed in Table 2, the tungstate catalyst was exposed to higher average radiations, both UV and visible, which explains its greater increase in photocatalytic activity when compared to the oxyiodide catalyst.

CONCLUSION

The results showed that different bismuth catalysts, active in visible light and with well-defined morphologies, were easily synthesized by a hydro/solvothermal method. For Bi_2WO_6 catalysts, the synthesis time and the addition of polyvinylpyrrolidone did not cause morphological differences in the samples, and calcination at 500 °C produced samples with smaller surface areas. For BiOI, microspheres with a larger surface area were obtained and the addition of PVP once again did not cause significant morphological difference. It did, however, promote greater activity. The $BiVO_4$ catalyst showed no satisfactory photocatalytic activity. Tests carried out in the presence of natural solar radiation showed that the bismuth catalysts are capable of degrading up to 98% of rhodamine dye. For the photocatalytic process using sunlight, two of the catalysts studied in this work proved to be viable alternatives. However, there is still a long way to go before this material is commercially available.

ACKNOWLEDGEMENTS

The authors acknowledge the financial support from CAPES and CNPq for this work.

REFERENCES

Alfaro, S. O. and Martínez-De La Cruz, A., Synthesis, characterization and visible-light photocatalytic properties of Bi_2WO_6 and $Bi_2W_2O_9$ obtained by co-precipitation method. Applied Catalysis A: General, 383(1–2), 128-133 (2010). https://doi.org/10.1016/j.apcata.2010.05.034

Bi, J., Che, J., Wu, L. and Liu, M., Effects of the solvent on the structure, morphology and photocatalytic properties of Bi_2MoO_6 in the solvothermal process. Materials Research Bulletin, 48(6), 2071-2075 (2013). https://doi.org/10.1016/j.materresbull.2013.02.033

Bonné, C., Pahwa, A., Picard, C. and Visseaux, M., Bismuth tris-silylamide: A new non-toxic metal catalyst for the ring opening (co-)polymerization of cyclic esters under smooth conditions. Inorganica Chimica Acta, 455, 521-527 (2017). https://doi.org/10.1016/j.ica.2016.06.027

Dai, X.-J., Luo, Y.-S., Zhang, W.-D. and Fu, S.-Y., Facile hydrothermal synthesis and photocatalytic activity of bismuth tungstate hierarchical hollow spheres with an ultrahigh surface area. Dalton Transactions, 39(14), 3426-3432 (2010). https://doi.org/10.1039/b923443h

Dong, S., Feng, J., Li, Y.,Hu, L., Liu, M., Wang, Y., Pi, Y.,Sun, J. and Sun, J., Shape-controlled synthesis of $BiVO_4$ hierarchical structures with unique natural-sunlight-driven photocatalytic activity. Applied Catalysis B: Environmental, 152, 413-424 (2014). https://doi.org/10.1016/j.apcatb.2014.01.059

Gamage Mcevoy, J., Cui, W. and Zhang, Z., Synthesis and characterization of Ag/AgCl–activated carbon composites for enhanced visible light photocatalysis. Applied Catalysis B: Environmental, 144, 702-712 (2014). https://doi.org/10.1016/j.apcatb.2013.07.062

Ge, M. and Liu, L., Sunlight-induced photocatalytic performance of Bi_2WO_6 hierarchical microspheres synthesized via a relatively green hydrothermal route. Materials Science in Semiconductor Processing, 25, 258-263 (2014). https://doi.org/10.1016/j.mssp.2013.12.026

Guang, L., Fei, W. and Xuejun, Z., Hydrothermal synthesis of m-$BiVO_4$ and m-$BiVO_4$/BiOBr with various facets and morphologies and their photocatalytic performance under visible

light. Journal of Alloys and Compounds, 697, 417-426 (2017). https://doi.org/10.1016/j.jallcom.2016.11.243

Hu, J., Weng, S., Zheng, Z., Pei, Z., Huang, M. and Liu, P., Solvents mediated-synthesis of BiOI photocatalysts with tunable morphologies and their visible-light driven photocatalytic performances in removing of arsenic from water. Journal of Hazardous Materials, 264, 293-302 (2014). https://doi.org/10.1016/j.jhazmat.2013.11.027

Huang, Y., Kang, S., Yang, Y., Qin, H., Ni, Z., Yang, S. and Li, X., Facile synthesis of Bi/Bi_2WO_6 nanocomposite with enhanced photocatalytic activity under visible light. Applied Catalysis B: Environmental, 196, 89-99 (2016). https://doi.org/10.1016/j.apcatb.2016.05.022

Huo, Y., Zhang, J., Miao, M. and Jin, Y., Solvothermal synthesis of flower-like BiOBr microspheres with highly visible-light photocatalytic performances. Applied Catalysis B: Environmental, 111-112, 334-341 (2012). https://doi.org/10.1016/j.apcatb.2011.10.016

Issarapanacheewin, S., Wetchakun, K.,Phanichphant, S., Kangwansupamonkon, W. and Wetchakun, N., Efficient photocatalytic degradation of Rhodamine B by a novel CeO_2/Bi_2WO_6 composite film. Catalysis Today, 278, 280-290 (2016). https://doi.org/10.1016/j.cattod.2015.12.028

Kaur, A. and Kansal, S. K., Bi2WO6 nanocuboids: An efficient visible light active photocatalyst for the degradation of levofloxacin drug in aqueous phase. Chemical Engineering Journal, 302, 194-203 (2016). https://doi.org/10.1016/j.cej.2016.05.010

Kim, S., Dong, W. J., Gim, S., Sohn, W., Park, J. Y., Yoo, C. J., Jang, H. W. and Lee, J.-L., Shape-controlled bismuth nanoflakes as highly selective catalysts for electrochemical carbon dioxide reduction to formate. Nano Energy, 39, 44-52 (2017). https://doi.org/10.1016/j.nanoen.2017.05.065

Kudo, A. and Hijii, S., H_2 or O_2 Evolution from Aqueous Solutions on Layered Oxide Photocatalysts Consisting of Bi^{3+} with 6s2 Configuration and d0 Transition Metal Ions. Chemistry Letters, 28(10), 1103-1104 (1999). https://doi.org/10.1246/cl.1999.1103

Li, Y., Liu, J., Huang, X. and Li, G., Hydrothermal Synthesis of Bi_2WO_6 Uniform Hierarchical Microspheres. Crystal Growth & Design, 7(7), 1350-1355 (2007). https://doi.org/10.1021/cg070343+

Lin, X., Liu, Z., Guo, X., Liu, C., Zhai, H.,Wang, Q. and Chang, L., Controllable synthesis and photocatalytic activity of spherical, flower-like and nanofibrous bismuth tungstates. Materials Science and Engineering: B, 188, 35-42 (2014). https://doi.org/10.1016/j.mseb.2014.06.005

Liu, Y., Ding, Z., Lv, H., Guang, J., Li, S. and Jiang, J., Hydrothermal synthesis of hierarchical flower-like Bi2WO6 microspheres with enhanced visible-light photoactivity. Materials Letters, 157, 158-162 (2015). https://doi.org/10.1016/j.matlet.2015.05.024

Liu, Z., Wu, B., Xiang, D. and Zhu, Y., Effect of solvents on morphology and photocatalytic activity of BiOBr synthesized by solvothermal method. Materials Research Bulletin, 47(11), 3753-3757 (2012). https://doi.org/10.1016/j.materresbull.2012.06.026

Lu, Y., Shang, H., Shi, F., Chao, C., Zhang, X. and Zhang, B., Preparation and efficient visible light-induced photocatalytic activity of m-BiVO4 with different morphologies. Journal of Physics and Chemistry of Solids, 85, 44-50 (2015). https://doi.org/10.1016/j.jpcs.2015.04.016

Ma, W., Li, Z. and Liu, W., Hydrothermal preparation of BiVO4 photocatalyst with perforated hollow morphology and its performance on methylene blue degradation. Ceramics International, 41(3), ,4340-4347 (2015). https://doi.org/10.1016/j.ceramint.2014.11.123

Meng, X. and Zhang, Z., Bismuth-based photocatalytic semiconductors: Introduction, challenges and possible approaches. Journal of Molecular Catalysis A: Chemical, 423, 533-549 (2016). https://doi.org/10.1016/j.molcata.2016.07.030

Mera, A. C., Contreras, D., Escalona, N. and Mansilla, H. D., BiOI microspheres for photocatalytic degradation of gallic acid. Journal of Photochemistry and Photobiology A: Chemistry, 318, 71-76 (2016). https://doi.org/10.1016/j.jphotochem.2015.12.005

Natarajan, K., Bajaj, H. C. and Tayade, R. J., Photocatalytic efficiency of bismuth oxyhalide (Br, Cl and I) nanoplates for RhB dye degradation under LED irradiation. Journal of Industrial and Engineering Chemistry, 34, 146-156 (2016). https://doi.org/10.1016/j.jiec.2015.11.003

Qin, X., Cheng, H., Wang, W., Huang, B., Zhang, X. and Dai, Y., Three dimensional BiOX (X=Cl, Br and I) hierarchical architectures: facile ionic liquid-assisted solvothermal synthesis and photocatalysis towards organic dye degradation. Materials Letters, 100, 285-288 (2013). https://doi.org/10.1016/j.matlet.2013.03.045

Ravidhas, C., Juliat Josephine, A., Sudhagar, P., Devadoss, A., Terashima, C., Nakata, K., Fujishima, A., Moses Ezhil Raj, A. and Sanjeeviraja, C., Facile synthesis of nanostructured monoclinic bismuth vanadate by a co-precipitation method: Structural, optical and photocatalytic properties. Materials Science in Semiconductor Processing, 30, 343-351 (2015). https://doi.org/10.1016/j.mssp.2014.10.026

Sivakumar, A., Murugesan, B., Loganathan, A. and Sivakumar, P., A review on decolourisation of dyes by photodegradation using various bismuth catalysts. Journal of the Taiwan Institute of Chemical Engineers, 45(5), 2300-2306 (2014). https://doi.org/10.1016/j.jtice.2014.07.003

Wu, D., Yue, S., Wang, W., An, T., Li, G., Yip, H. Y., Zhao, H. and Wong, P. K., Boron doped BiOBr nanosheets with enhanced photocatalytic inactivation of Escherichia coli. Applied Catalysis B: Environmental, 192, 35-45 (2016). https://doi.org/10.1016/j.apcatb.2016.03.046

Wu, J., Duan, F., Zheng, Y. and Xie, Y., Synthesis of Bi_2WO_6 Nanoplate-Built Hierarchical Nest-like Structures with Visible-Light-Induced Photocatalytic Activity. The Journal of Physical Chemistry C, 111(34), 12866-12871 (2007). https://doi.org/10.1021/jp073877u

Wu, S., Wang, C., Cui, Y., Wang, T., Huang, B., Zhang, X., Qin, X. and Brault, P., Synthesis and photocatalytic properties of BiOCl nanowire arrays. Materials Letters, 64(2), 115-118 (2010). https://doi.org/10.1016/j.matlet.2009.10.010

Xia, J., Yin, S., Li, H., Xu, H., Xu, L. and Zhang, Q., Enhanced photocatalytic activity of bismuth oxyiodine (BiOI) porous microspheres synthesized via reactable ionic liquid-assisted solvothermal method. Colloids and Surfaces A: Physicochemical and Engineering Aspects, 387(1–3), 23-28 (2011). https://doi.org/10.1016/j.colsurfa.2011.07.023

Xiao, X., Xing, C., He, G., Zuo, X.,Nan, J. and Wang, L., Solvothermal synthesis of novel hierarchical Bi4O5I2 nanoflakes with highly visible light photocatalytic performance for the degradation of 4-tert-butylphenol. Applied Catalysis B: Environmental, 148, 154-163 (2014). https://doi.org/10.1016/j.apcatb.2013.10.055

Yang, T., Xia, D., Chen, G. and Chen, Y., Influence of the surfactant and temperature on the morphology and physico-chemical properties of hydrothermally synthesized composite oxide BiVO4. Materials Chemistry and Physics, 114(1), 69-72 (2009). https://doi.org/10.1016/j.matchemphys.2008.08.005

Yu, J., Xiong, J., Cheng, B., Yu, Y. and Wang, J., Hydrothermal preparation and visible-light photocatalytic activity of Bi_2WO_6 powders. Journal of Solid State Chemistry, 178(6), 1968-1972 (2005). https://doi.org/10.1016/j.jssc.2005.04.003

Zhang, G., Li, M., Yu, S., Zhang, S., Huang, B. and Yu, J., Synthesis of nanometer-size Bi_3TaO_7 and its visible-light photocatalytic activity for the degradation of a 4BS dye. Journal of Colloid and Interface Science, 345(2), 467-473 (2010a). https://doi.org/10.1016/j.jcis.2010.01.084

Zhang, G., Lü, F., Li, M., Yang, J., Zhang, X. and Huang, B., Synthesis of nanometer Bi_2WO_6 synthesized by sol–gel method and its visible-light photocatalytic activity for degradation of 4BS. Journal of Physics and Chemistry of Solids, 71(4), 579-582 (2010b). https://doi.org/10.1016/j.jpcs.2009.12.041

Zhang, L., Chen, D. and Jiao, X. Monoclinic Structured BiVO4 Nanosheets: Hydrothermal Preparation, Formation Mechanism, and Coloristic and Photocatalytic Properties. The Journal of Physical Chemistry B, 110(6), 2668-2673 (2006). https://doi.org/10.1021/jp056367d

Zhang, L., Wang, W., Chen, Z., Zhou, L., Xu, H. and Zhu, W., Fabrication of flower-like Bi_2WO_6 superstructures as high performance visible-light driven photocatalysts. Journal of Materials Chemistry, 17(24), 2526-2532 (2007). https://doi.org/10.1039/b616460a

Zhang, Y., Zhang, N., Tang, Z.-R. and Xu, Y.-J. Identification of Bi_2WO_6 as a highly selective visible-light photocatalyst toward oxidation of glycerol to dihydroxyacetone in water. Chemical Science, 4(4), 1820-1824 (2013). https://doi.org/10.1039/c3sc50285f

Zhao, G., Liu, W., Li, J., Lv, Q., Li, W. and Liang, L., Facile synthesis of hierarchically structured $BiVO_4$ oriented along (010) facets with different morphologies and their photocatalytic properties. Applied Surface Science, 390, 531-539 (2016). https://doi.org/10.1016/j.apsusc.2016.08.126

Zhou, L., Wang, W., Liu, S., Zhang, L., Xu, H. and Zhu, W., A sonochemical route to visible-light-driven high-activity $BiVO_4$ photocatalyst. Journal of Molecular Catalysis A: Chemical, 252(1–2), 120-124 (2006). https://doi.org/10.1016/j.molcata.2006.01.052

Zhou, L., Wang, W. and Zhang, L. Ultrasonic-assisted synthesis of visible-light-induced Bi_2MO_6 (M = W, Mo) photocatalysts. Journal of Molecular Catalysis A: Chemical, 268(1–2), 195-200 (2007). https://doi.org/10.1016/j.molcata.2006.12.026

Zhu, Z., Du, J., Li, J., Zhang, Y. and Liu, D. An EDTA-assisted hydrothermal synthesis of $BiVO_4$ hollow microspheres and their evolution into nanocages. Ceramics International, 38(6), 4827-4834 (2012). https://doi.org/10.1016/j.ceramint.2012.02.071